

## Removal of a food dye on two solid supports by adsorption

### Remoção de um corante alimentar em dois suportes sólidos por adsorção

Abderezak Guemache<sup>1</sup> , Fares Kakoul<sup>1</sup> , Louanes Hamzioui<sup>1</sup> , Bouacha Samir<sup>1</sup> 

### ABSTRACT

Activated carbon and natural clay are extremely promising for the removal of dyes in a water solution. Natural clay and activated carbon were characterized using X-ray diffraction (XRD) and Fourier-transform infrared spectroscopy (FTIR) techniques, and the food dye was characterized by UV-Visible. The effects of various experimental parameters, such as initial carmine concentration, contact time, temperature and pH were studied. The removal of the dye increases with the decrease in the initial concentration of carmine and the contact time of the solution. The percentage of carmine removal increases accordingly, reaching 97% for activated carbon and 67% for natural clay. Langmuir and Freundlich adsorption models were used for the adsorption equilibrium descriptions. The data was very well corrected with these models. Monolayer adsorption capacities were equal to 31 mgg<sup>-1</sup> at pH 8.0 and 27°C. Adsorption measurements show that the adsorption process is very fast and physical in nature. Thermodynamic parameters such as enthalpy  $\Delta H^\circ$ ,  $\Delta S^\circ$  entropy and  $\Delta G^\circ$  free enthalpy were also evaluated to reveal the nature of adsorption. The results explain that the adsorption process is an exothermic, spontaneous physisorption.

**Keywords:** carmine; removal; activated carbon; clay natural; XRD; FTIR; adsorption isotherm, thermodynamic parameters.

### RESUMO

O carvão ativado e a argila natural são excepcionalmente promissores para a remoção de corantes em solução em água. Argila natural e carvão ativado foram caracterizados utilizando técnicas de difração de raios X DRX e espectrofotometria FTIR (*Fourier-transform infrared*), o corante alimentar foi caracterizado por UV-Visível. Foram estudados os efeitos de vários parâmetros experimentais, como concentração inicial de carmin, tempo de contato, temperatura e pH. A remoção do corante aumenta com a diminuição da concentração inicial de carmin e do tempo de contato da solução. A porcentagem de remoção de carmin aumenta proporcionalmente, chegando a 97% para o carvão ativado e 67% para a argila natural. Os modelos de adsorção de Langmuir e Freundlich foram utilizados para as descrições do equilíbrio de adsorção. Os dados foram muito bem corrigidos com esses modelos. As capacidades de adsorção em monocamada foram iguais a 31 mgg<sup>-1</sup> em pH 8,0 e 27°C. Medições de adsorção mostram que o processo de adsorção é muito rápido e de natureza física. Parâmetros termodinâmicos como entalpia  $\Delta H^\circ$ , entropia  $\Delta S^\circ$  e entalpia livre  $\Delta G^\circ$  também foram avaliados para revelar a natureza da adsorção. Os resultados explicam que o processo de adsorção é uma fisissorção exotérmica e espontânea.

**Palavras-chave:** carmin; remoção; carvão ativado; argila natural; XRD; FTIR; isotermia de adsorção; parâmetros termodinâmicos.

<sup>1</sup>University of M'Sila – M'Sila, Algeria.

Correspondence address: Guemache Abderezak, Laboratory of Water, Environment and Renewable Energies, Faculty of Technology, University of M'sila – PO Box 166 – Ichbilila, Postal Code: 28000 – M'Sila, Algeria. E-mail: abderezak.guemache@univ-msila.dz

Conflicts of interest: the authors declare no conflicts of interest.

Funding: none.

Received on: 08/30/2023. Accepted on: 10/18/2023.

<https://doi.org/10.5327/Z2176-94781614>



This is an open access article distributed under the terms of the Creative Commons license.

## Introduction

Water is the source of life on Earth, and it is not possible to imagine the existence of life without water, and all our activities, our industries and our food depend entirely on its availability. But due to the great expansion of the industrial activities that the world is facing today and the various pollutants resulting from it, obtaining clean water has become extremely difficult, on the one hand. On the other, environmental degradation caused by polluted water has become a real problem that cannot be ignored.

Dyes are classified into three main classes: 1. anionic: direct dyes, acids and reagents, 2. cationic: all base dyes, and 3. non-ionic dyes: disperse dyes. Carmine dyes are used in food additives under number E120 to give a red color (Silva et al., 2021). Removal of effluent color is one of the most difficult of the requirements of textile finishing, dye manufacturing, and pulp and paper industries. These industries are water consumers and therefore cause water pollution. Most of these dyes are harmful when they have contact with living tissues for a long time (Purkait et al., 2007).

Dyes are one of the most common water pollutants, as textile dyes alone account for 17 to 20% of industrial pollutants (Müller-Maatsch, 2016). Of course, dyes are not only used in the textile industry, but also in almost all industries, from paper and plastic manufacturing to the food that we eat, and all of them are not without color (Coulate and Blackburn, 2018). So the pollution caused by it will be in huge quantities, but the problem does not lie in the quantities, but in the effects resulting from that. Due to the presence of toxic chemicals used in the manufacture of dyes, exposure to these substances has devastating effects on living organisms and human health, in addition to distorting the landscape (Dione et al., 2018).

Since pigments have a high ability to dissolve in water, adsorption is considered one of the most common and effective methods of treating the resulting pollution, and many adsorbent materials are used for this purpose, especially activated carbon because of its properties (Otto et al., 2021), in addition to the use of clay, as it is one of the most abundant and cheapest materials (Dhar et al., 2023), and it impacted the ecological balance. Therefore, treating pollution with dyes is essential and extremely important, and there are several ways to do this, including filtration and sedimentation processes, ion exchange, adsorption, aerobic and anaerobic treatment, and other physical and chemical methods (Saravanan et al., 2021).

The competitiveness of an adsorbent can be studied by analyzing isotherms adsorption data, which can be obtained by a series of experimental laboratory tests (Das and Mondal, 2011). The modelling of isotherms adsorption data is an indispensable means to calculate and compare adsorption performance, which is essential for the optimization of adsorption pathways of mechanisms, expression of adsorbent capabilities and effective adsorption design systems (Ki, 2023).

The most important properties include the maximum adsorption capacity ( $q_m$ ), which can be found by adsorption kinetics. The adsorp-

tion kinetics can be exploited to evaluate the solute absorption rate, used to verify the equilibrium time, as well as to unveil the time required for the adsorbent and adsorbent interaction to be preserved. Kinetic parameters are important because they are used as a means of estimating the size and transfer rate of industrial equipment adsorption systems (Farias et al., 2022).

Carmine is the hydrated aluminum chelate of carminic acid (EC, 2018). It is commonly obtained by precipitating carminic acid in aluminum hydroxide in the form of aluminum or aluminum-calcium salt (Lim et al., 2014). Because of this, carmines are carminic acid aluminum lakes in which aluminum and carminic acid are believed to be disclosed in the molar ratio 1:2 (EC, 2018), stable at all pH values above 3.5, approximately, as well as heat, light and oxygen.

In this note we will study the adsorption of carmine dye on the surface of two different materials: activated carbon and clay, where we will observe how the adsorption process is affected by changing the dye concentration, the mass of the adsorbents, the temperature, and the pH and contact time.

## Experimental process

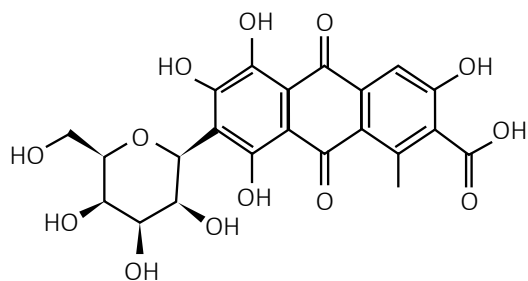
Carmine is a bright red pigment that can be obtained from carminic acid, which is produced by some scale insects, such as cochineal. Carmine pigment is used in the manufacture of food colorings, medicines and cosmetics (Feketea and Tsabouri, 2017). Eleven adsorption treatments were performed, based on the adsorption methodologies used by several authors (Wang et al., 2011; Auta and Hameed, 2014).

The adsorbate used was carmine dye in solution with an initial concentration of  $2,510^{-3} \text{ molL}^{-1}$  and molar mass of  $492.38 \text{ g mol}^{-1}$ . In this work, the experimental methodology for the study of the adsorption of carmine dye on activated carbon and clay will be explained, and we will present the tools, devices and materials necessary to conduct this study, in addition to explaining how to collect and analyze samples. The effect of changes in concentration, temperature and pH will also be studied, and its effect on adsorption capacity, as well as all the results obtained, will be shown.

## Materials

### Dye used

A carmine (Neutral dye) (Figure 1), Carmine is a bright red pigment that can be obtained from carminic acid, which is produced by some scale insects such as cochineal. Carmine pigment is used in the manufacture of food colorings, medicines and cosmetics, and many other uses. A stock solution of carmine dye at a concentration of  $2,510^{-3} \text{ molL}^{-1}$  was prepared by dissolving 625 mg dye powder in 500 mL of bi-distilled water, and then daughter solutions were placed in 5mL test tubes at a mass concentration of 62 mg to 625  $\text{mgL}^{-1}$ .



$C_{22}H_{20}O_{13}$  Molecular Weight 492,386 4g/mol

Figure 1 – Chemical structure of carmine.

### Method of analysis

At the end of each adsorption experiment, the adsorbent was removed by Büchner filtration. Then the filtrate obtained was analyzed by UV-visible spectrophotometry by monitoring the changes in absorbance at  $\lambda_{\max}=493$  nm for carmine. The amount adsorbed is calculated using the following formula: The amount of carmine adsorbed on clay and activated carbon,  $Q_e$  (mg L<sup>-1</sup>), was evaluated using the following Equation 1:

$$Q_e = (C_0 - C_e) * V/M \quad (1)$$

Where:

$C_0$  and  $C_e$  (mg L<sup>-1</sup>) referred to the initial value and the equilibrium concentration of carmine, respectively;

$V$  (L) is the volume of the carmine solution;

$M$  (g) is the mass of the Clay and activated carbon.

The adsorption (percentage) with the  $C_i$  and  $C_e$  was calculated according to the following Equation 2:

$$\%T = \frac{(C_i - C_e)}{C_i} * 100 \quad (2)$$

### Characterization techniques

#### Adsorbent used

The physical-chemical characteristics of the materials were determined using standard procedures (Singh et al., 2017). The application of natural and abundant adsorbents, such as raw clay and activated charcoal for water treatment, is an authorized route to protect the water capital. Several techniques were used. The resulting phase analysis was performed by recording the X-ray diffracts of grams of powder through a Xpert Pro (Panalytical) diffract meter using the  $CuK\alpha$  radiation of copper ( $\lambda=1.5418\text{\AA}$ ) and infrared spectroscopy. The raw clay, dried at 100°C/24h, was analyzed by infrared Fourier transform spectroscopy on a SHIMADZU FTIR-8000 spectrometer. The two solids were prepared as a solid mixture (KBr mixture) and analyzed by absorption.

## Results and Discussion

### Material chemical analysis

#### X-ray diffraction (XRD)

The spectrum presented in Figure 2 makes it possible to identify the structure. Figure 2 shows the diffractogram of the raw clay. According to the XRD diagram obtained, the clay has a mineralogical composition and inter-layer distances practically identical to bentonite (Boukhemkhem, Pizarro and Molina, 2020).

The preparation of the natural clay was also undertaken through the procedure described by Kaya and Yukselen (2005), and Liu et al. (2008) (Table 1).

From Figure 2 we can see: the natural clay is characterized by four peaks. The first is located at 15.037 $\text{\AA}$  (001) and the other three are at 4.479 $\text{\AA}$  (110), 2.567 $\text{\AA}$  (200) and 1.498 $\text{\AA}$  (001). This diffracts gram shows that the non-clay minerals present in varying amounts from one sample to another are mainly quartz with characteristic reflections at  $d_{001}=3.35\text{\AA}$  and 4.28 $\text{\AA}$ , calcite ( $d_{001}=3.21\text{\AA}$ ), and feldspars ( $d_{001}=4.06\text{\AA}$ ) (Zhu et al., 2007). We also observe in the same Figure 2, the XRD diffractogram of the activated carbon, the presence of a large peak ( $2\Theta=32^\circ$ ) indicating an amorphous structure (Senthilkumar et al., 2011).

#### FTIR Analysis

#### Spectra for natural clay

The FTIR tests confirmed that the analyzed materials have a crystalline structure. The spectra obtained are illustrated by Figure 3. We note: the band that spans between 1600–1700  $\text{cm}^{-1}$  may be attributed to the valence vibrations of the OH group of the constituent water, in addition to the binding vibrations of the adsorbed water located at 1631  $\text{cm}^{-1}$ . An absorption band center on 3624  $\text{cm}^{-1}$  is due to the valence vibrations of the OH groups bound to the octahedral Al cations (Al-OH-Al) (El Kassimi et al, 2021). The Si-O bond is characterized by the intense band located between 900–1200  $\text{cm}^{-1}$  and center around 1008.9  $\text{cm}^{-1}$  corresponds to the valence vibrations of the Si-O bond (Adel, Ahmed and Mohamed, 2021). The bands at 768  $\text{cm}^{-1}$  and 411-500  $\text{cm}^{-1}$  are assigned to Si-O-Al and Si-O-Mg, Si-O-Fe and bending vibrations, respectively.

The bands are between 800 and 1008  $\text{cm}^{-1}$ , coming from the Si-O-Al bond. Another characteristic band for bending vibrations of adsorbed water usually appears at 1600–1631  $\text{cm}^{-1}$  as a medium band.

#### Spectra for carmine

In the FTIR spectroscopic analysis of carmine (Figure 4), a broad band appeared at 3400  $\text{cm}^{-1}$  representing the OH group. The peak observed at 1697  $\text{cm}^{-1}$  was assigned to a ketonic bond (C=O). The peak observed at 2931  $\text{cm}^{-1}$  was assigned to stretching of CH bond. The peak observed at 1639  $\text{cm}^{-1}$  was assigned to a carbon-carbon double bond (C=C). The band observed at 1615–1410  $\text{cm}^{-1}$  was assigned to the vibration of aromatic rings.

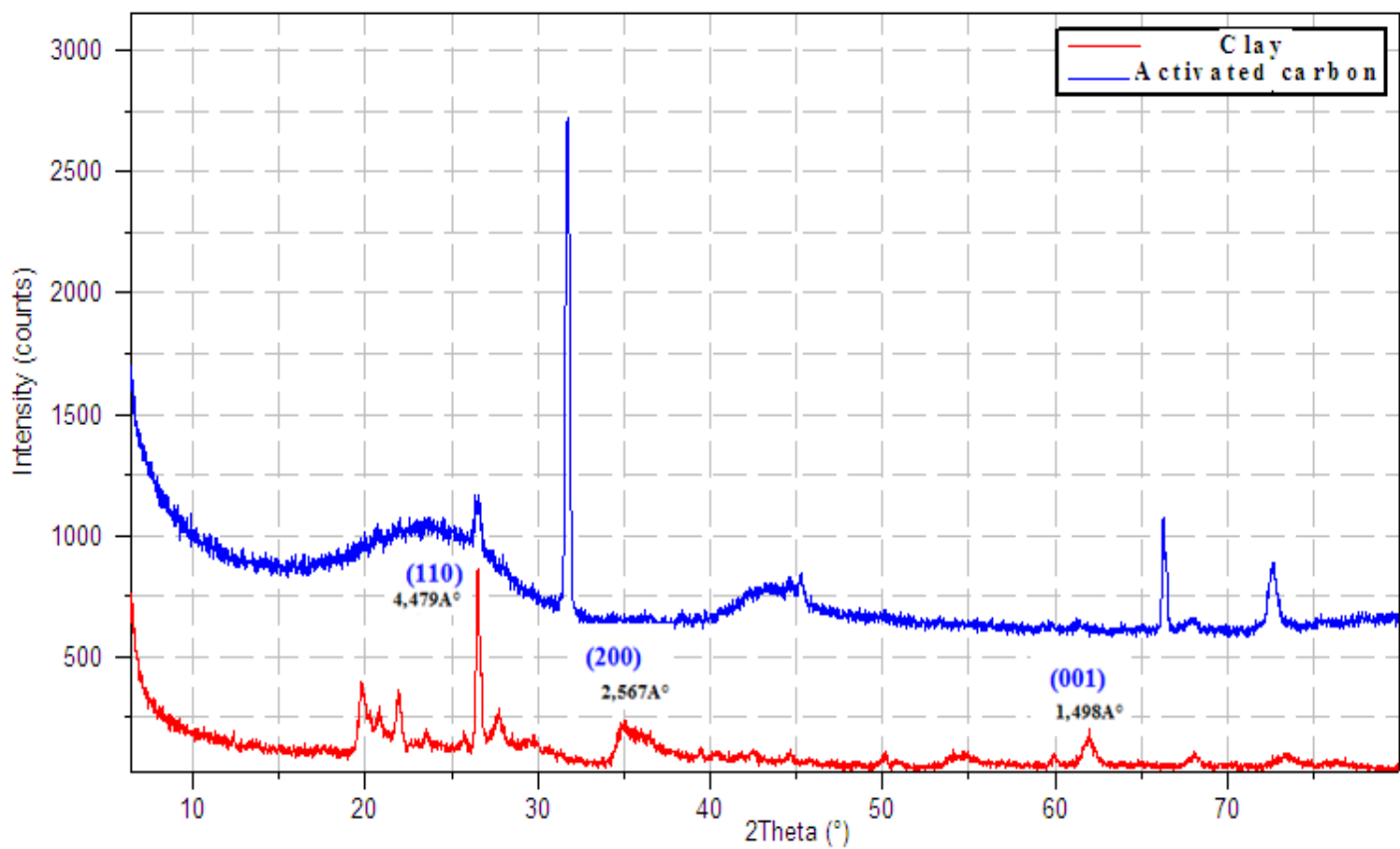


Figure 2 – Diffractogram of natural clay and activated carbon.

Table 1 – Chemical composition of natural clay.

Elements	%
SiO <sub>2</sub>	54.92
Al <sub>2</sub> O <sub>3</sub>	16.92
Fe <sub>2</sub> O <sub>3</sub>	1.95
MnO	0.02
MgO	4.29
CaO	0.71
Na <sub>2</sub> O	1.23
K <sub>2</sub> O	0.73
TiO <sub>2</sub>	0.05
P <sub>2</sub> O <sub>5</sub>	0.13

The band observed at 1350–400 cm<sup>-1</sup> was an infrared fingerprint region in which the peaks indicated a stretching vibration of single degree of freedom vibration.

#### Plotting the calibration curve (UV-Visible)

Solutions with different concentrations (0.5–5 mgL<sup>-1</sup>) were prepared from the standard stock solution. Using a spectrophotome-

ter, the absorbance of the primary dye solution was measured, and the maximum wavelength was obtained,  $\lambda_{max}=493$  nm (Figure 5). Then we measured the absorbance of the dilute standard solutions at the previous wavelength to obtain the calibration curve (Latif, Abdullah and Saleem, 2016).

#### Initial concentration effect

To do this, we put a fixed mass of activated carbon,  $m=100$  mg, in each of the standard solutions of the dye with different initial concentrations (625, 312, 62 mg) and a volume of 5 mL at a constant pH and temperature, and after the end of the experiment the samples are placed in a centrifuge for 5 minutes at 2500 rpm. Then we filter the solutions and measure the absorption ratio with a spectrophotometer and calculate the adsorption ratio after that, and the same previous steps for the bentonite clay. The following Figure 6 shows the results:

Where we note that the higher the initial concentration, the greater the adsorption capacity to reach a maximum value at the highest concentration (30 mgg<sup>-1</sup> for activated carbon and 10 mgg<sup>-1</sup> for clay, at a concentration of 623 mgL<sup>-1</sup>). We can also note the difference in the adsorption capacity between activated carbon and bentonite clay as it is greater in the first as compared to the second.

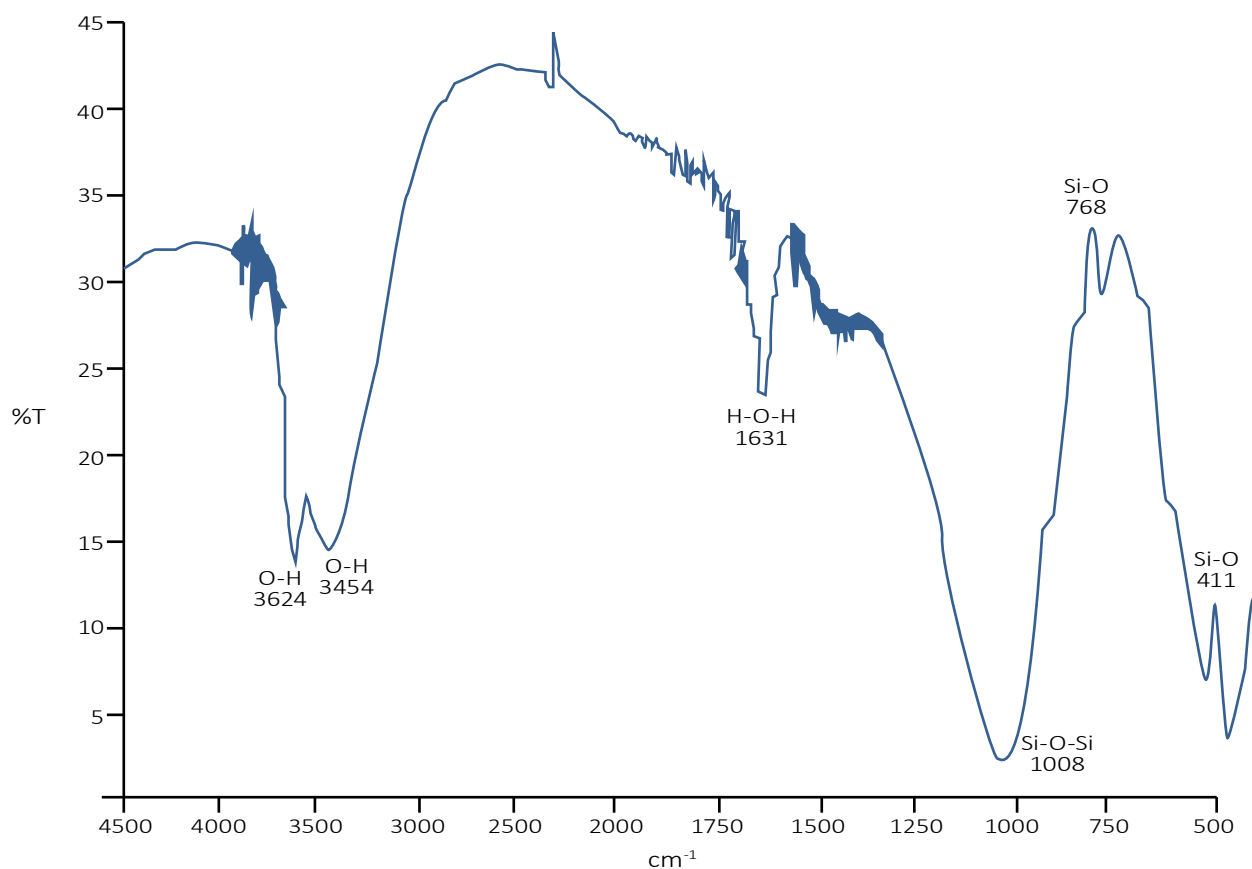


Figure 3 – FTIR spectra for natural clay.

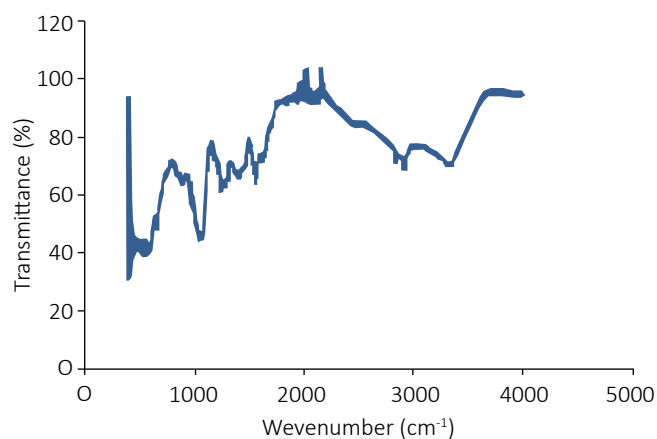


Figure 4 – FTIR spectra for carmine.

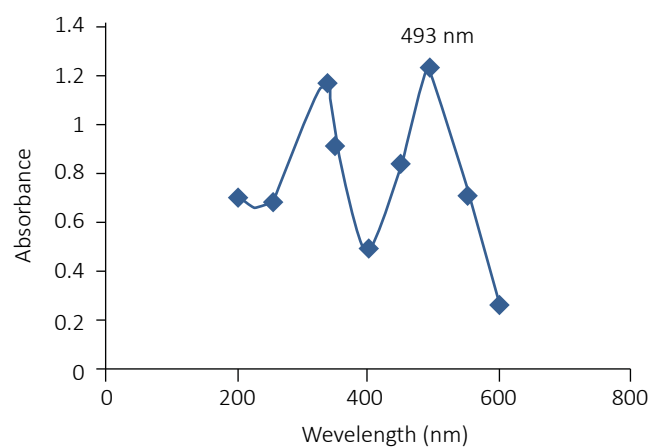


Figure 5 – Absorbance and calibration curves of carmine.

This result is due to the fact that the large concentration of the dye in the solution necessarily means a larger number of molecules, which will increase the number of collisions between it and the surface of the adsorbent material, and thus enhance the chance of bonding to its

surface, unlike low concentrations. In addition, the large adsorption capacity of activated carbon compared to clay is due to its large surface area, which can absorb more pollutant particles than clay (El Maataoui et al., 2019).

*The effect of contact time*

To measure the effect of contact time, we prepared the solutions in the same way as before, where we put a fixed mass of activated carbon,  $m=100$  mg, with different concentrations of dye, pH value and constant temperature, and we measured the results during different time periods (2, 4, 6, 8, 24 h), where the lowest concentration corresponds to the lowest period of time, and the same for clay. After placing the samples in a centrifuge, filtering them and measuring the absorbance, we obtained the results represented in Figure 7.

As the contact time increases, the adsorption capacity increases, and we also notice a similarity in the adsorption capacity between activated carbon and bentonite clay in the range of low dye concentrations, but soon the contrast appears between them in the range of large concentrations and the longer contact time. This is due to the fact that the adsorption process does not occur immediately, since in porous materials adsorption occurs first on the available sites on the outer surface, and then on the surface of the inner pores, which takes a longer time (Joseph et al., 2010).

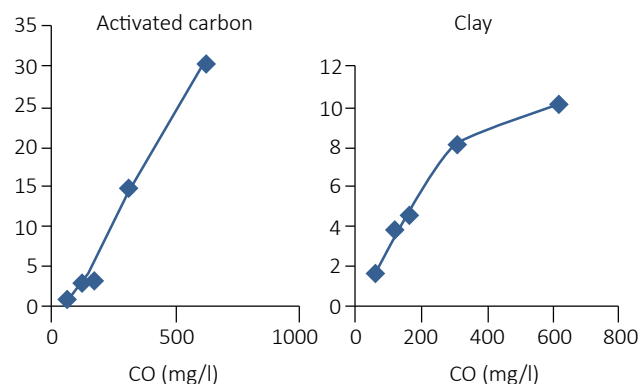


**Figure 6 – Initial concentration effect.**

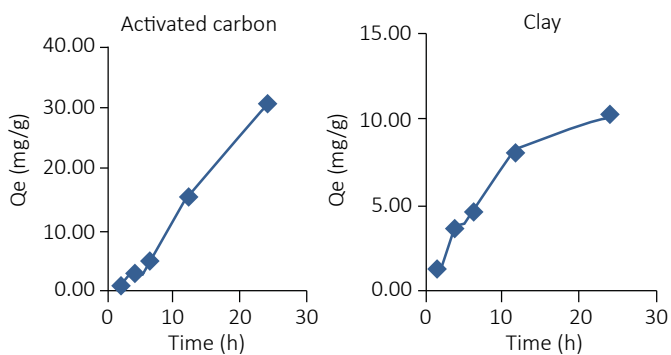


**Figure 7 – Effect of contact time.**

*The effect of changing the pH*

To do this, we put a fixed mass of activated carbon,  $m=0.025$  g, in 5 mL of the dye solution at a constant concentration of  $155$   $\text{mgL}^{-1}$ , at a constant time and temperature, and at different pH values (4, 6, 10), and in the same way for the clay. After placing the samples in a centrifuge, filtering them and measuring the absorbance, we obtained the results represented in Figure 8.

As for clay, we can observe an increase in the adsorption capacity, with a raise in the pH value in the range [4,6], which then tends to settle at a value close to  $\text{mgg}^{-1}$  in the moderate and basic range. When it comes to activated carbon, the adsorption capacity appears to be more stable with the change in pH, as the value of the adsorption capacity in the acidic, moderate and basic ranges is close to  $30$   $\text{mgg}^{-1}$ , with a slight increase in the acidic range. In addition, there is a discrepancy in the adsorption capacity between carbon activated and bentonite clay and that are in the acidic range where they are greater in carbon compared to clay (Cuba et al., 2020).

The reason for the weak adsorption capacity in the acidic field is the presence of hydrogen ions  $\text{H}^+$  of a large amount that competes with the dye molecules for adsorption sites (Mittal, Al Alili and Alhassan, 2020). In addition, clay is more affected by these ions due to the properties of clay, that differs from activated carbon in terms of the nature of the charges on its surface (Adeyemo, Adeoye and Bello, 2017). We note the absence of this effect when there are no hydrogen ions in the moderate and basic range, where the adsorption capacity is large and more stable.

*The effect of changing the temperature*

To measure the effect of temperature on the adsorption process, we prepared standard solutions with a volume of 5 mL and with different concentrations, and put a different mass for each solution, where the lowest mass of carbon corresponds to the lowest concentration of the dye solution. We put the previous solutions at different temperatures (25, 30, 35, 40, 45 degrees), where the lowest temperature corresponds to the lowest concentration, and in the same way with the bentonite clay.

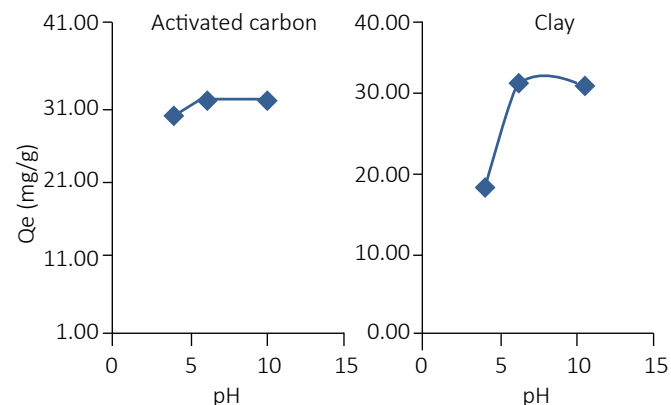


**Figure 8 – The effect of changing the pH.**

After placing the samples in a centrifuge, filtering them and measuring the absorbance, we obtained the results represented in Figure 9.

In relation to the general form of the curve, we can notice that the adsorption capacity decreases with the increasing temperature, where it was 22 mgg<sup>-1</sup> at 25 degrees and reached 11 mgg<sup>-1</sup> at 45 degrees for clay. As for activated carbon, the maximum adsorption capacity was 45 mgg<sup>-1</sup> at a temperature of 30 degrees, to reach 30 mgg<sup>-1</sup> at 45 degrees. We can also note the discrepancy in the adsorption capacity between activated carbon and bentonite clay as it is larger in carbon compared to clay. The reason for the decrease in the adsorption capacity with increasing temperatures is the fact that the adsorption process is an exothermic process. In addition, the molecules at high temperatures have a high kinetic energy (Fuj and Wang, 2015), which reduces the chance of having them on the surface of the adsorbent material.

*Decolorization Ratio (T %)*

To identify the most efficient adsorbent material for removing color, be it activated carbon or clay, we will determine the percentage of color removal for both, and then make a comparison. In order to do this, we will use the same data from the experiment through which we determined the effect of the initial concentration (a fixed mass of the adsorbent with variable dye concentrations), obtaining the following Figure 10.

Through the curve, we can make several observations: for activated carbon, we note that its efficiency in removing the dye increases as its concentration is raised to reach 97% at the highest concentration. For clay, we can notice in general that its efficiency in removing the dye decreases with the increase in the initial concentration of the dye, where it was 62% at its highest value, at a concentration of 125 mgL<sup>-1</sup>, to decrease to 32% at the highest concentration of 623 mgL<sup>-1</sup>.

We can also note that the curve is divided into two parts: the range of minimum concentrations, which ends at a value close to 200 mgL<sup>-1</sup>, and the other range, which is for major concentrations, starting

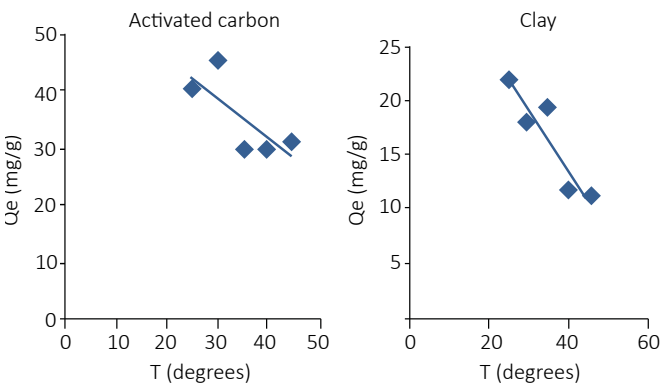


Figure 9 – The effect of changing the temperature.

from the previous value and ending at the maximum concentration. We can see that the decolorization efficiency for clay is high in the first range compared to activated carbon, while the opposite is in the second range, where the efficiency of the clay decreases significantly in exchange for the significant increase in the efficiency of activated carbon.

This is due to the large surface area of activated carbon that allows it to absorb a large amount of colorant, while the surface area of clay is less than it is in carbon, and therefore absorbs a smaller amount of dye. As for the range of small concentrations, the clay’s high efficiency in removing color may be due to the charges on its surface that cause ion exchange with the dye molecules (Hassan and Carr, 2018), which quickly run out to return its efficiency to decline with large concentrations.

*Adsorption isotherms*

Adsorption isotherms help us know the nature of adsorption, and whether it is a monolayer or multilayer (or physical or chemical adsorption). For this purpose, we will use solutions with different concentrations ranging from 62 mgL<sup>-1</sup> to 625 mgL<sup>-1</sup>, with a variable mass of adsorbent, and after obtaining the results we will draw a graph of the two functions (Equations 3 and 4):

$$\text{Log } C_e = f(\text{log } C_e) \tag{3}$$

$$Q_e = f\left(\frac{1}{C_e}\right) \tag{4}$$

From the curves, we will obtain the values of the constants of the two adsorption isotherms that we will use (Equations 5 and 6):

**Freundlich equation:**

$$\text{Log } Q_e = \text{log } K_f + \frac{1}{n} \text{log } C_e \tag{5}$$

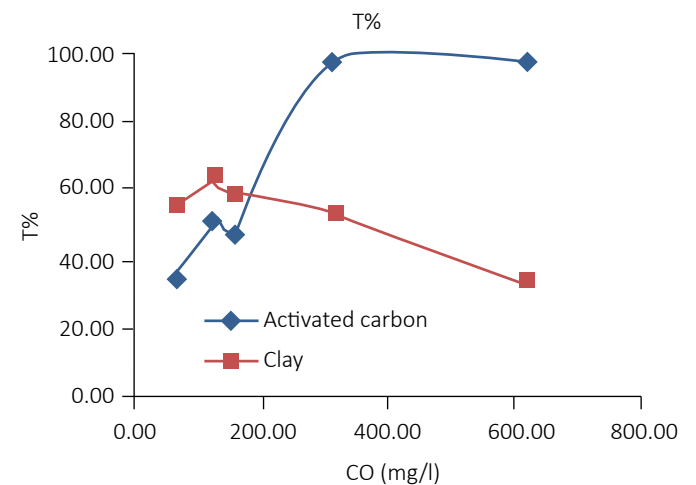


Figure 10 – Decolorization.

**Langmuir equation:**

$$Q_e = 1/Q_m + 1/K * 1/Q_m * \frac{1}{C_e} \tag{6}$$

Where:

C<sub>e</sub>: Equilibrium solute residual concentration (mgL<sup>-1</sup>);

Q<sub>m</sub>: Maximum adsorption capacity (m<sub>g</sub>g<sup>-1</sup>);

k<sub>L</sub>: Adsorption equilibrium constant for the solute/adsorbent(Lm<sub>g</sub><sup>-1</sup>);

k<sub>f</sub> and n: constants that are characteristic of the efficiency of an adsorbent with respect to a given solute.

We get the following curves: the Freundlich model predicts that the dye concentration on the adsorbent will increase as long as there is an increase in dye concentration in the liquid phase. However, experimental evidence indicates that an isotherm plateau is reached at a limited value of the solid phase concentration. This tray is not predicted by the Freundlich equation. Therefore, the equation itself has no real physical significance (Figure 11) (Allen, McKay and Khader, 1988).

The Langmuir adsorption isotherm is used to describe the balance between the adsorbate and the adsorbent system, where adsorption of adsorbate is limited to a molecular layer at or before a relative unit pressure is reached. Although the isotherm originally proposed by Langmuir in 1918 is generally appropriate to describe the chemisorption process when ionic or covalent chemical bonds are formed between adsorbent and adsorbate (Figure 12).

Through these curves, we were able to obtain the constants of the Langmuir and Freundlich isotherms, which are represented by the following values (Table 2).

After calculating the correlation coefficients and the constants of the Freundlich and Langmuir equation, we can say that, in both cases, for either the Freundlich or the Langmuir isotherm, and for either activated carbon or clay, the previous two models do not fully describe adsorption (based on correlation coefficients), which can be justified for the Freundlich isotherm by the fact that it describes adsorption very precisely at small concentrations, while it fails in large concentrations (Maurya and Mittal, 2010).

But in all cases we can determine which of the two models is more appropriate to describe adsorption. As for clay, we can notice that the correlation coefficient of the Freundlich model is 0.816 while in the Langmuir model it is 0.511, and this means that the first is more suitable to describe the adsorption of carmine pigment on the clay, which leads to the conclusion that the adsorption is multi-layered or physical, characterizing the irregular surfaces (Langmuir, 1918). For activated carbon, we find that the correlation coefficient for the Freundlich model is 0.736, while in the Langmuir model it is 0.768 (Crombie-QUILTY and McLoughlin, 1983).

This means that the Langmuir model is more suitable to describe the adsorption of carmine dye on activated carbon, as this model describes the monolayer adsorption, which characterizes homogeneous surfaces (Gao et al., 2013).

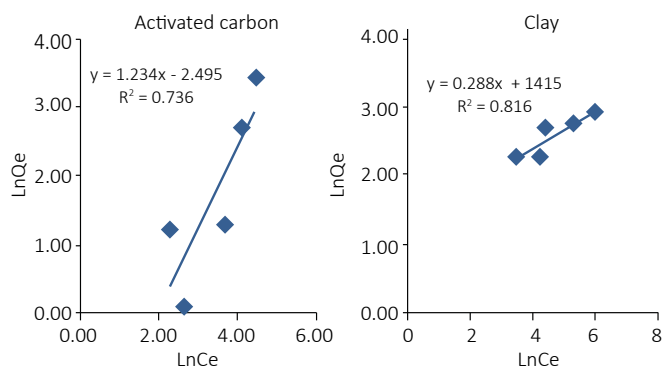


**Figure 11 – Freundlich isotherm.**

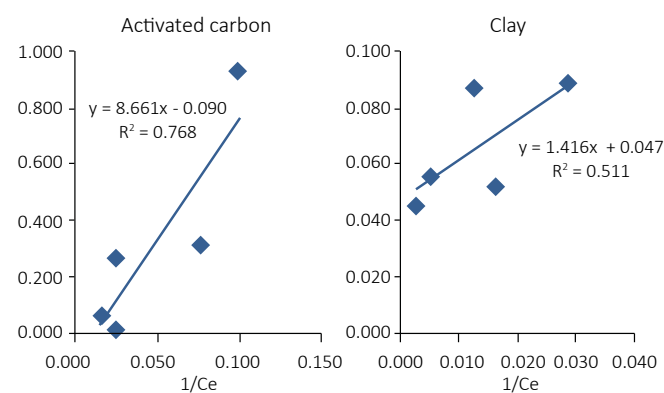


**Figure 12 – Langmuir isotherm.**

**Table2 – Isotherm parameters obtained from the fit of various equations.**

Isotherm models	Activated Carbon	Clay
<b>Langmuir</b>	$1/Q_e = 1/Q_m + 1/K * 1/Q_m * 1/C_e$	
Q <sub>e</sub> (m <sub>g</sub> g <sup>-1</sup> )	31±0.2	30±0.01
K <sub>L</sub> (Lm <sub>g</sub> <sup>-1</sup> )	0.01±0.0	0.033±0.05
R <sup>2</sup>	0.768	0.511
<b>Freundlich</b>	$Q_e = K C_e^{1/n}$	
Q <sub>e</sub> (m <sub>g</sub> g <sup>-1</sup> )	31±0.2	11±0.01
K <sub>f</sub> (m <sub>g</sub> g <sup>-1</sup> )	0.082±0.05	4.11±0.01
n	0.810±0.15	3.47±0.01
R <sup>2</sup>	0.736	0.816



## Adsorption thermodynamics

### Thermodynamic parameters

The thermodynamic parameters for the adsorption of carmine by natural and activated clay such as the enthalpy ( $\Delta H^0$ ), the Gibbs free energy change ( $\Delta G^0$ ) and the entropy change ( $\Delta S^0$ ) can be calculated from the variation of maximum adsorption with temperature (T) using the following basic thermodynamic relations (Staroń, et al., 2017).

Figure 13 shows the proposed adsorption mechanism of carmine molecules onto the surface of natural clay. Other factors, such as porosity, temperature, pH, etc., are also responsible for the effective adsorption of dyes (Equations 7 and 8).

$$\ln K_d = -\frac{\Delta H^0}{RT} + \frac{\Delta S}{R} \quad (7)$$

$$\ln K_d = \Delta G^0/RT \quad (8)$$

According to Equation 7, the mean value of the enthalpy change due to the adsorption of phenol by natural and activated clay over the temperature range studied can be determined graphically by the linear plotting of  $\ln K_d$  against  $1/T$  (Ahmad et al., 2021), using the least squares analysis shown in Figure 14.

The average development of enthalpy can be determined from the slope of the straight line. Gibbs free energy deviation and entropy change with temperature can be calculated using Equations 7, 8, 9 and 10, successively, and the results are arranged in Table 3.

$$\Delta S^0 = (\Delta H^0 - \Delta G^0)/T \quad (9)$$

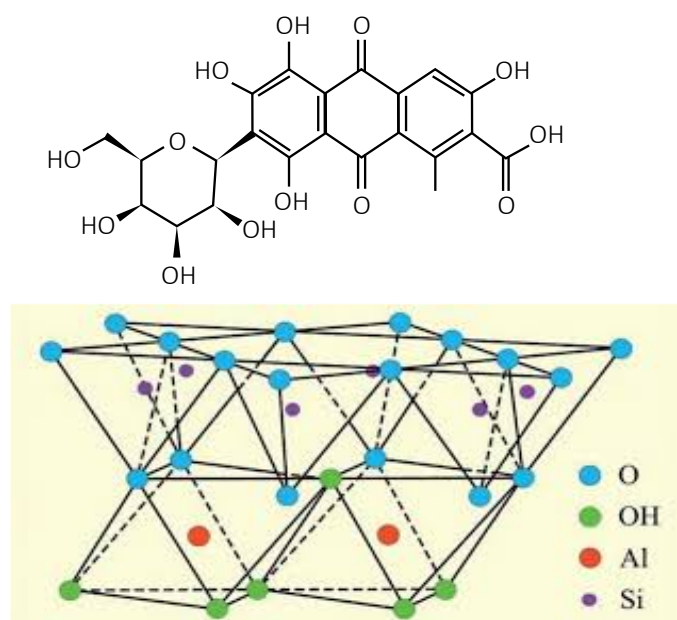


Figure 13 – Proposed adsorption mechanism of carmine molecules onto the surface of natural clay.

$$K_d = Q_e/C_e \quad (10)$$

An important result that can be obtained from Table 3 is that the free energy of Gibbs ( $\Delta G^0$ ) is small and negative, with its value decreasing with the increase in temperature. This indicates that the processes of adsorption of carmine by natural clay and activated carbon can be optimized by decreasing the temperature. Entropy change values ( $\Delta S^0$ ) are positive and remain almost constant with temperature.

This shows that structural changes in carmine, natural clay and activated carbon develop during the adsorption process, as per Figure 14. Negative values of enthalpy change ( $\Delta H^0$ ) for adsorption are less than  $52 \text{ kJ mol}^{-1}$ , which suggests the physical nature of sorption, that is, physisorption, conducted with van der Waals forces.

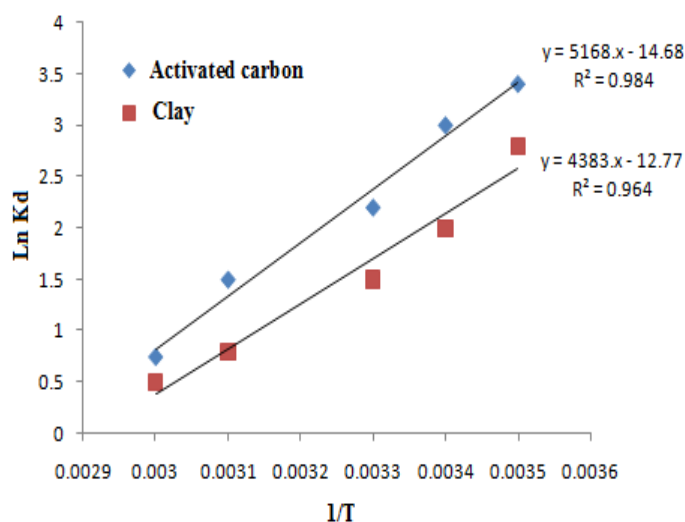


Figure 14 – Van'tHott equation for adsorption of carmine on activated carbon and natural clay at different temperatures.

Table 3 – The thermodynamic parameters for the adsorption of carmine on natural clay and activated carbon.

Thermodynamic parameters			
	$\Delta H^0$ (kJ/mole) mean value	$\Delta G^0$ (kJ/mole)	$\Delta S^0$ (KJ/mole) mean value
<b>Activated carbon</b>			
293K	-0.52	-1.789	4.399
303K		-3.695	
323K		-9.190	
<b>Natural Clay</b>			
293K	-0.44	1.191	2.563
303K		3.695	
323K		6.5641	

The adsorption enthalpy change ( $\Delta H^0$ ) is  $-0.52$  and  $-0.44 \text{ kJ mol}^{-1}$ , indicating physical adsorption of carmine on natural clay and activated carbon (Seki and Yurdakoc, 2006). The overall adsorption process appears to be exothermic.

## Conclusions

In this research, we studied the adsorption process of food dye carmine, on the surface of activated carbon and natural clay. First, we characterized adsorbate and adsorbents by spectral analyses to identify the presence of a chemical bond from a spectrum. Second, to compare the adsorption efficiency of each of them under initial conditions, we estimated the adsorption capacity at different initial concentrations, at different temperatures, at different pH values, and at different contact times. Third, we studied the kinetics and thermodynamics of carmine adsorption on the two adsorbents through two isotherms models, which are the Freundlich model and the Langmuir model, thus, estimating the thermodynamic parameters ( $\Delta H^0$ ,  $\Delta G^0$ ,  $\Delta S^0$ ).

The results showed that the textures of clay and activated carbon, according to spectral analyses, have chemical bonds that are capable of

exerting attraction forces on the surface, to generate interactions that retain the adsorbate on the surface of the adsorbent. In addition, the study of the effect of contact time, the effect of temperature and the effect of pH on the adsorption process showed results to the effect that activated charcoal is more effective than clay in the range of large dye concentrations. Therefore, activated carbon and natural clay can be considered excellent adsorbents, depending on the initial conditions, vis-à-vis the adsorption capacity, which reaches its maximum value and remains stable over time.

Regarding isotherms adsorption models, we find that the Freundlich model is more suitable for clay, while the Langmuir model is more suitable for activated carbon, from which we can conclude that clay is a better adsorbate at low concentrations, whereas this is true for activated coal at high concentrations.

The thermodynamic properties of a system are statistical averages corresponding to many molecules. The energy of a solute molecule varies as it approaches the surface to reach a minimum at a certain distance, near an adsorption site. According to thermodynamic quantities, the adsorption of carmine on the surface of natural clay and activated carbon is exothermic.

## Contribution of authors

GUEMACHE, A.: data curation, formal analysis, investigation, methodology, software, validation, visualization, writing – original draft. HAMZIOUI, L.: data curation, formal analysis, visualization, writing – original draft. KAHOU, F.: conceptualization, methodology, supervision, writing – review & editing, funding, acquisition, project administration, resources. SAMIR, B.: writing – review & editing.

## References

- Adel, M.; Ahmed, M.A.; Mohamed, A.A., 2021. Effective removal of indigo carmine dye from wastewaters by adsorption onto mesoporous magnesium ferritenanoparticles. *Environmental Nanotechnology, Monitoring & Management*, v. 16, 100550. <https://doi.org/10.1016/j.enmm.2021.100550>
- Adeyemo, A.A.; Adeoye, I.O.; Bello, O.S., 2017. Adsorption of dyes using different types of clay: a review. *Applied Water Science*, v. 7, (2), 543-568. <https://doi.org/10.1007/s13201-015-0322-y>
- Ahmad, M.B.; Soomro, U.; Muqet, M.; Ahmed, Z., 2021. Adsorption of Indigo Carmine dye onto the surface-modified adsorbent prepared from municipal waste and simulation using deep neural network. *Journal of Hazardous Materials*, v. 408, 124433. <https://doi.org/10.1016/j.jhazmat.2020.124433>
- Allen, S.J.; McKay, G.; Khader, K.Y.H., 1988. Multi-component sorption isotherms of basic dyes onto peat. *Environmental Pollution*, v. 52, (1), 39-53. [https://doi.org/10.1016/0269-7491\(88\)90106-6](https://doi.org/10.1016/0269-7491(88)90106-6)
- Auta, M.; Hameed, B.H., 2014. Chitosan-clay composite as highly effective and low-cost adsorbent for batch and fixed-bed adsorption of methylene blue. *Chemical Engineering Journal*, v. 237, 352-361. <https://doi.org/10.1016/j.cej.2013.09.066>
- Boukhemkhem, A.; Pizarro, A.H.; Molina, C.B., 2020. Enhancement of the adsorption properties of two natural bentonites by ion-exchange: equilibrium, kinetics and thermodynamic study. *Clay Minerals*, v. 55, (2), 132-141. <https://doi.org/10.1180/clm.2020.19>
- Coultrate, T.; Blackburn, R.S., 2018. Food colorants: their past, present and future. *Coloration Technology*, v. 134, (3), 165-186. <https://doi.org/10.1111/cote.12334>
- Crombie-Quilty, M.B.; McLoughlin, A.J., 1983. The adsorption of bovine serum albumin by activated sludge. *Water Research*, v. 17, (1), 39-45. [https://doi.org/10.1016/0043-1354\(83\)90284-1](https://doi.org/10.1016/0043-1354(83)90284-1)
- Cuba, R.M.F.; Paiva, D.C.A.C.; Cintra, T.S.; Terán, F.J.C., 2020. Influence of inorganic phosphorus and ph value on the removal of aqueous environment glyphosate-based formulation by adsorption. *Brazilian Journal of Environmental Sciences*, v. 55, (1), 48-60. <https://doi.org/10.5327/Z2176-947820200557>
- Das, B.; Mondal, N.K., 2011. Calcareous soil as a new adsorbent to remove lead from aqueous solution: equilibrium, kinetic and thermodynamic study. *Universal Journal of Environmental Research & Technology*, v. 1, (4), 515-530. eISSN 2249 0256
- Dhar, A.K.; Himu, H.A.; Bhattacharjee, M.; Mostufa, M.G.; Parvin, F., 2023. Insights on applications of bentonite clays for the removal of dyes and heavy metals from wastewater: a review. *Environmental Science and Pollution Research*, v. 30, (3), 5440-5474. <https://doi.org/10.1007/s11356-022-24277-x>

- Dione, C.T.; Diagne, I.; Ndiaye, M.; Diebakate, C.; Ndiaye, B.; Diop, A., 2018. Contamination métallique d'une espèce de poisson de la côte dakaraise. *European Scientific Journal*, v. 14, (12), 374-383. <https://doi.org/10.19044/esj.2018.v14n12p374>
- El Kassimi, A.; Achour, Y.; El Himri, M.; Laamari, R.; El Haddad, M., 2021. Removal of two cationic dyes from aqueous solutions by adsorption onto local clay: experimental and theoretical study using DFT method. *International Journal of Environmental Analytical Chemistry*, 1-22. <https://doi.org/10.1080/03067319.2021.1873306>
- El Maataoui, Y.; M'rabet, E.; Maaroufi, A.; Dahhour, A., 2019. Spiramycin adsorption behavior on activated bentonite, activated carbon and natural phosphate in aqueous solution. *Environmental Science and Pollution Research*, v. 26, (16), 1595315972. <https://doi.org/10.1007/s11356-019-05021-4>
- European Commission (EC), 2018. COMMISSION REGULATION (EU) 2018/1472 of 28 September 2018 amending Annex II to Regulation (EC) No 1333/2008 of the European Parliament and of the Council and the Annex to Commission Regulation (EU) No 231/2012 as regards Cochineal, Carminic acid, Carmines. *Off J Eur Union*. 247:1-4.
- Fuj, C.; Wang, M., 2015. Adsorption of methylene blue by a high-efficiency adsorbent (polydopaminemicrospheres): Kinetics, isotherm, thermodynamics and mechanism analysis. *Chemical Engineering Journal*, v. 259, 5361. <https://doi.org/10.1016/j.cej.2014.07.101>
- Feketea, G.; Tsabouri, S., 2017. Common food colorants and allergic reactions in children: myth or reality. *Food Chemistry*, v. 230, 578-588. <https://doi.org/10.1016/j.foodchem.2017.03.043>
- Farias, J.P.; Demarco, C.F.; Afonso, T.F.; Aquino, L.S.; Vieira, M.L.G.; Cadaval Junior, T.R.; Quadro, M.S.; Andrezza, R., 2022. Comparison of the adsorption kinetics of methylene blue using rice husk ash activated with different chemical agents. *Brazilian Journal of Environmental Sciences*, v. 57, (2), 279-289. <https://doi.org/10.5327/Z2176-94781195>
- Gao, Z.P.; Yu, Z.F.; Yue, T. L.; Quek, S.Y., 2013. Adsorption isotherm, thermodynamics and kinetics studies of polyphenols separation from kiwifruit juice using adsorbent resin. *Journal of Food Engineering*, v. 116, (1), 195201. <https://doi.org/10.1016/j.jfoodeng.2012.10.037>
- Hassan, M.M.; Carr, C.M., 2018. A critical review on recent advancements of the removal of reactive dyes from dyehouse effluent by ion-exchange adsorbents. *Chemosphere*, v. 209, 201-219. <https://doi.org/10.1016/j.chemosphere.2018.06.043>
- Joseph, S.D.; Camps-Arbestain, M.; Lin, Y.; Munroe, P.; Chia, C.H.; Hook, J.; van Zwieten L.; Kimber, S.; Cowie, A.; Singh, B.P.; Lehmann, J.; Foidl, N.; Smernik, R.J.; Amonette, J.E., 2010. An investigation into the reactions of biochar in soil. *Soil Research*, v. 48, (7), 501-515. <https://doi.org/10.1071/SR10009>
- Kaya, A.; Yukselen, Y., 2005. Zeta potential of soils with surfactants and its relevance to electrokinetic remediation. *Journal of Hazardous Materials*, v. 120, (1-3), 119-126. <https://doi.org/10.1016/j.jhazmat.2004.12.023>
- Ki, E.L.S., 2023. Removal of dye using powdered activated carbon coated on polyurethane foam. Doctoral Dissertation, Universiti Tunku Abdul Rahman. Retrieved 2023-12-15, from <http://eprints.utar.edu.my/id/eprint/5582>
- Langmuir, I., 1918. The adsorption of gases on plane surfaces of glass, mica and platinum. *Journal of the American Chemical Society*, v. 40, (9), 1361-1403. <https://doi.org/10.1021/ja02242a004>
- Latif, I.K.; Abdullah, H.M.; Saleem, M.H., 2016. Magnetic conductive hydrogel nanocomposites as drug carrier. *Nanoscience and Nanotechnology*, v. 6, (3), 48-58. <https://doi.org/10.5923/j.nn.20160603.03>
- Lim, H.-S.; Choi, J.-C.; Song, S.-B.; Kim, M., 2014. Quantitative determination of carmine in foods by high-performance liquid chromatography. *Food Chemistry*, v. 158, 521-526. <https://doi.org/10.1016/j.foodchem.2014.02.122>
- Liu, R.; Frost, R.L.; Martens, W.N.; Yuan, Y., 2008. Synthesis, characterization of mono, di and tri alkyl surfactant intercalated Wyoming montmorillonite for the removal of phenol from aqueous systems. *Journal of Colloid and Interface Science*, v. 327, (2), 287-294. <https://doi.org/10.1016/j.jcis.2008.08.049>
- Maurya, N.S.; Mittal, A.K., 2010. Biosorptive color removal: applicability of equilibrium isotherm models. *Practice Periodical of Hazardous, Toxic, and Radioactive Waste Management*, v. 14, (1), 25-36. [https://doi.org/10.1061/ASCE1090-025X201014:1\(25\)](https://doi.org/10.1061/ASCE1090-025X201014:1(25))
- Mittal, H.; Al Alili, A.; Alhassan, S.M., 2020. High efficiency removal of methylene blue dye using  $\kappa$ -carrageenan-poly (acrylamide-co-methacrylic acid)/AQSOA-Z05 zeolite hydrogel composites. *Cellulose*, v. 27, (14), 8269-8285. <https://doi.org/10.1007/s10570-020-03365-6>
- Müller-Maatsch, J.; Gras, C., 2016. 18 - The "Carmine Problem" and Potential Alternatives, *Handbook on Natural Pigments in Food and Beverages, Industrial Applications for Improving Food Color*, Woodhead Publishing Series in Food Science, Technology and Nutrition, 385-428. <https://doi.org/10.1016/B978-0-08-100371-8.00018-X>
- Otto, I.M.; Morselli, L.B.G.A.; Bunde, D.A.B.; Pieniz, S.; Quadro, M.S.; Andrezza, R., 2021. Adsorption of methylene blue dye by different methods of obtaining shrimp residue chitin. *Brazilian Journal of Environmental Sciences*, v. 56, (4), 589-598. <https://doi.org/10.5327/Z217694781170>
- Purkait, M.K.; Maiti, A.; Dasgupta, S.; De, S., 2007. Removal of congo red using activated carbon and its regeneration. *Journal of Hazardous Materials*, v. 145, (1-2), 287-295. <https://doi.org/10.1016/j.jhazmat.2006.11.021>
- Saravanan, A.; Kumar, P.S.; Jeevanantham, S.; Karishma, S.; Tajsabreen, B.; Yaashikaa, P.R.; Reshma, B., 2021. Effective water/wastewater treatment methodologies for toxic pollutants removal: processes and applications towards sustainable development. *Chemosphere*, v. 280, 130595. <https://doi.org/10.1016/j.chemosphere.2021.130595>
- Seki, Y.; Yurdakoc, K., 2006. Adsorption of promethazine hydrochloride with KSF montmorillonite. *Adsorption*, v. 12, (1), 89-100. <https://doi.org/10.1007/s10450-006-0141-4>
- Senthilkumar, S.T.; Senthilkumar, B.; Balaji, S.; Sanjeeviraja, C.; Selvan, R.K., 2011. Preparation of activated carbon from sorghum pith and its structural and electrochemical properties. *Materials Research Bulletin*, v. 46, (3), 413-419. <https://doi.org/10.1016/j.materresbull.2010.12.002>
- Silva, L.J.; Pereira, A.R.; Pereira, A.M.; Pena, A.; Lino, C.M., 2021. Carmines (E120) in coloured yoghurts: a case-study contribution for human risk assessment. *Food Additives & Contaminants: Part A*, v. 38, (8), 1316-1323. <https://doi.org/10.1080/19440049.2021.1923820>
- Singh, M.; Sarkar, B.; Hussain, S.; Ok, Y. S.; Bolan, N.S., 2017. Influence of physico-chemical properties of soil clay fractions on the retention of dissolved organic carbon. *Environmental Geochemistry and Health*, v. 39, (6), 1335-1350. <https://doi.org/10.1007/s10653-017-9939-0>
- Staroń, P.; Chwastowski, J.; Banach, M., 2017. Sorption and desorption studies on silver ions from aqueous solution by coconut fiber. *Journal of Cleaner Production*, v. 149, 290-301. <https://doi.org/10.1016/j.jclepro.2017.02.116>
- Wang, L.; Zhang, J.; Wang, A., 2011. Fast removal of methylene blue from aqueous solution by adsorption onto chitosan-g-poly (acrylic acid)/attapulgite composite. *Desalination*, v. 266, (1-3), 33-39. <https://doi.org/10.1016/j.desal.2010.07.065>
- Zhu, L.; Zhu, R.; Xu, L.; Ruan, X., 2007. Influence of clay charge densities and surfactant loading amount on the microstructure of CTMA-montmorillonite hybrids. *Colloids and Surfaces A: Physicochemical and Engineering Aspects*, v. 304, (1-3), 41-48. <https://doi.org/10.1016/j.colsurfa.2007.04.019>